Chalak Qazani, Mohammad Reza, Bidabadi, Behrooz Shirani, Asadi, Houshyar, Nahavandi, Saeid, and Bidabadi, Farnoosh Shirani (2023) ***Multiobjective optimization of roll-forming procedure using NSGA-II and type-2 fuzzy neural network*****. IEEE Transactions on Automation Science and Engineering, 21 (3) pp. 3842-3851.**

https://doi.org/10.1109/TASE.2023.3287921

Multiobjective Optimisation of roll-forming Procedure Using NSGA-II and Type-2 Fuzzy Neural Network

Mohammad Reza Chalak Qazani[1,2], Behrooz Shirani Bidabadi[3], Houshyar Asadi[2], Saeid Nahavandi[2], Farnoosh Shirani Bidabadi[4]

***Abstract*—In this research, the effective indexes in the cold roll-forming procedure that can affect the energy utilization and required maximum torque of the forming line have been investigated and optimised using NSGA-II and type-2 fuzzy neural networks. The effective parameters were strip thickness, bending angle increment, flange width, inter-distance between the rolling stands and bending radius. Recently, traditional machine-learning applications have been employed in roll-forming technology for different purposes, such as prediction of web-warping, energy efficiency, and strip breakage. A finite element model (FEM) roll-forming procedure was utilised to extract the appropriate datasets for this study. type-2 fuzzy neural network (T2FNN) is not employed in cold roll-forming technology. In this study, T2FNN is employed to imitate the dynamic model of the cold roll-forming procedure to estimate energy consumption and torque. In the following, the NSGA-II extracts the optimal cold roll-forming procedure parameters to reach the lowest energy consumption and maximum torque as the process's most economical solution. The proposed model is designed and developed under MATLAB software. Fourteen optimal solutions are suggested based on the extracted Pareto-Front of the NSGA-II using the T2FNN of the process.**

***Note to Practitioners*—In this research, a hybrid machine-learning method is designed and developed with a combination of T2FNN and NSGA-II to extract the optimal roll-forming procedure parameters to reach the lowest usage of energy as well as the lowest requirement of maximum torque. Implementing the proposed method in cold roll-forming production lines can save millions of dollars in massive factories by reducing the usage of energy and the emission of greenhouse gases. The proposed algorithm is quite fast. Then there is no need for high graphic computers for real-time implementation of the proposed method.**

***Index Terms*—cold roll-forming, torque/energy consumption, type-2 fuzzy neural network, Multiobjective optimisation, NSGA-II.**

I. Introduction

Cold roll-forming procedure is the most common method in producing steel pipes and profiles. In this process, the continuous steel strip goes through multiples forming a stand. A pair of rolls in each stand bend incrementally [1]. The forming process continues on the successive forming stand until the last forming stand, where the final shape of the profile comes out of the forming line [2]. Since the forming process is progressive and the strip is formed gradually through a couple of successive forming stages, the process is complicated. Many parameters can affect the process, energy consumed, and product features. Therefore, accurate control of the parameters needs to be considered. Otherwise, the efficiency will drop significantly [3]. Since a large portion of steel rolls in the world is turned into steel pipes, profiles and tubes, an investigation around energy optimisation of energy expenditure in the cold roll-forming procedure can save a significant amount of energy.

So far, several studies have investigated the energy and torque consumed in the cold roll-forming procedure. Lindgren [4] studied the influence of materials' strength on the roll loads and torques in the roll-forming procedure and extracted a couple of equations to calculate the load and power consumed by the roll-forming line. He found that the more materials' strength, the more power and load required to form the steel strip. Shirani Bidabadi *et al.* [5] investigated the required torque on each forming stand to deform the steel strip to produce a U-shape profile in the cold roll-forming procedure. His numerical results had good agreement with the experiments. He divided the effective parameters into two groups, including the parameters related to the geometry of the product and the ones related to the roll-forming line. Then they sorted out the influence of each parameter on the required torque to form the steel strip. Shirani Bidabadi *et al.* [6] also investigated the influence of roll-forming product geometry and the roll-forming line features on the energy consumption of production. They found that the bend angle increment (BAI) is the main effective parameter in changing energy consumption. Traub and Groche [7] investigated the effect of the rotational speed of the shaft in each stand on the energy demand in the roll-forming procedure. Using finite element model (FEM) simulation, they predicted the energy saving of the roll-forming procedure up to 51%. They found a positive impact in their experiments as well. Then, they developed a rule-based method to enhance the

(*Corresponding author: Mohammad Reza Chalak Qazani*)
M. R. C. Qazani is with the Faculty of Computing and Information Technology, Sohar University, Sohar, 311, Oman (e-mail: m.r.chalakqazani@gmial.com)
M. R. C. Qazani, H. Asadi and Saeid Nahavandi are with the Institute for Intelligent Systems Research and Innovation, Deakin University, Geelong, VIC 3216, Australia (e-mail: m.r.chalakqazani@gmial.com; houshyar.asadi@deakin.edu.au; saeid.nahavandi@deakin.edu.au)
B. Shirani Bidabadi is with the Department of Mechanical Engineering, Texas A&M University, Texas 77843, USA (e-mail: behrooz.shirani@tamu.edu)
F. Shirani Bidabadi is with the Department of computer Science & engineering, Texas A&M University, Texas 77843, USA (e-mail: farnoosh.shirani@tamu.edu)

energy efficiency of the process [8]. Davoodi *et al.* [9] investigated the effect of the Yield strength of the materials, strip thickness (ST) and forming angle increment on the roll torque and force in the roll-forming procedure. They predicted a decrease in the applied force and torque when yield strength, trip thickness, and a decrease in increment angle. Paralikas *et al.* [10] introduced the energy performance indicator in the U-section roll-forming procedure. They categorised a variety of parameters based on their efficacy on energy consumption. They found that BAI, line velocity, and internal distance between the forming stands (I-D) are the most influential among other parameters. They also tried optimising the roll-forming line's energy efficiency using hybrid modelling [11]. They concluded that roll gap, roller radius and BAI had the dominant effect on energy efficiency.

Deep learning and machine-learning techniques have recently been developed in different research fields like materials microstructure, manufacturing, and energy [12-14]. They have gained a remarkable interest across Industry 4.0. The machine-learning-based models are designed and developed using the experimental datasets of the process. They often are more accurate than the classical models [15]. One of the pioneer studies in using the machine-learning method in roll-forming technology was conducted by Pican *et al.* [16]. They estimated the roll force during temper rolling considering 12 process parameters. They used a feedforward neural network (NN) with two hidden layers to develop their network. At the same time, there are 48 neurons in the first hidden layer and 24 neurons in the second hidden layer. The margin of error between the practical results and their proposed machine-learning method was 13.2%. Cho *et al.* [17] proposed a hybrid mathematical and feedforward NN to predict the tandem cold mill rolling load. Their proposed feedforward NN consists of one hidden layer and 12 neurons. Vannucci *et al.* [18] calculated the flow stress within the hot rolling of steel using seven hidden layers' feedforward NN s for real-time applications. Calvo-Rolle *et al.* [19] proposed the intelligent PID controller in the roll-forming procedure to optimise the process by improving the permanent regimes and transient response. Dadgar Asl *et al.* [20] used single hidden layer feedforward NN with 39 neurons to estimate the required torque of the roll-forming procedure via the regenerated FEM datasets. Their dataset consists of 32 data, then they trained their proposed feedforward NN using 28 data and tested using the 4 data. The margin of error between their proposed machine-learning method and FEM results during the testing process was 0.27%. Lachwar *et al.* [21] classified the different types of mill scales of hot rolling mills using a decision tree, support vector machine, and NN. They [21] discovered that the decision tree is the most accurate model for classifying the mill scales. Rath *et al.* [22] calculated the flow stress of hot-rolling steel mills using the experimental datasets. They used a single hidden layer feedforward NN and four neurons. The main advantage of their proposed method was the comparable accuracy because of the fewer neurons. Zhang and Jiang [23] used deep learning methods to decrease the massive energy usage of CNC machines in online applications. Xiao *et al.* [24] extracted the optimal turning flexible machining parameters using eta-reinforcement learning. A comparative analysis is followed to prove the efficiency of their proposed method. Yucel *et al.* [25] employed Bayesian linear regression, Gaussian process regression and linear regression to extract the mechanical properties of the cold roll-forming HSLA steels using microstructure statistics. Using a recurrent NN, Chen et al. [26] investigated strip breakage in cold rolling. They implemented the first deep learning method in the cold roll-forming procedure. Woo *et al.* [26] used support vector regression and a genetic algorithm to optimise the roll-forming procedure with less web warping. The support vector regression calculates the web warping based on speed, height, and BAI. Then, a genetic algorithm is employed to extract the optimal process parameters to reach the minimum web warping. Xiao *et al.* [27] accomplished a comparative study higher efficiency of the machine-learning method in decreasing the energy consumption in the machining process. Soleymani *et al.* [28] implemented the convolutional NN and transfer learning in the thread rolling process to predict the micro-hardness of the final product. Xia *et al.* [29] used feedforward neural networks to calculate the rolling power, force and slip in the tandem cold rolling process. Recently, Zhu *et al.* [30] investigate the implementation of machine learning method on three-dimensional (3D) surface forming. They used DeepFit algorithm to extract the spring back in 3D surface bending process in order to consider the uncertainty of the process. Also, Cao *et al.* [31] calculate the curvature of roll bended profile using extreme gradient boosting (XGBoost).They also used error compensation network and Bayesian optimisation method to increase the accuracy of their proposed method.

According to the literature [15-32], the current paper aims to build an efficient machine-learning method to calculate the energy consumption and torque in the roll-forming procedure using a type-2 fuzzy neural network (T2FNN). T2FNNs have not been used to extract the optimal process parameters in a roll-forming process. It should be noted that feedforward neural networks [16-18, 20-22], decision trees [21], support vector machines [21, 26], deep learning [23], reinforcement learning [24], traditional machine-learning [25, 27], and recurrent neural network [32] are used before to extract the model which is capable of imitating the behaviour of the roll-forming process. However, a Type-2 fuzzy neural network has not been investigated in this domain, which is the main novelty of this study. A type-2 fuzzy neural network is employed in this study as:

1. It can easily handle uncertainty with a dynamic optimal learning problem.
2. It has strong estimation power to accurately identify the system.
3. Unlike type-1, the secondary membership in type-2 fuzzy neural networks is also a fuzzy set. Then, type-2 fuzzy systems have one more degree of freedom.

There are two methods for capturing the dataset for training and testing purposes of the soft computing methods, including experimental setups and FEM. The experimental study is expensive and time taking. In contrast, FEM can be used as the alternative way to extract the dataset easier than holding the real experiment. It should be noted that the required dataset for training and testing of the employed machine-learning method in this study is extracted using the FEM environment with selections of different inputs, including the BAI at each stand, I-D, ST, channel flange width (FW), and corner radius.

Using the type-2 fuzzy model increases the accuracy of the model facing the uncertainty part of the process. In addition, the combination of NNs and fuzzy systems, known as T2FNN, can decrease the training and testing process of the system for the implementation of online applications. It should be noted that it is the first time that T2FNN has been employed for modelling the roll-forming procedure. In addition, the extracted T2FNN model is employed inside the Multiobjective genetic algorithm (NSGA-II) to extract the optimal solution of the process resulting in less torque and energy consumption during the operation. It should be noted that NSGA-II is one of the pioneers in the area of Multiobjective optimization to extract the optimal parameters of the complex system in different sectors, such as the roll-forming process. In recent studies, NSGA-II is employed for extracting the optimal solution in multiple cost functions in finance, biology, cloud computing, energy, etc. [33-36].

The overview of the cold roll-forming, including the preparation of the FEM and the extraction of the datasets, is explained in Section II. The introduced methodology using the combination of the T2FNN, and NSGA-II is explained in Section III. In Section IV, the results are extracted and discussed under MATLAB software. The conclusions are made in Section V.

II. Cold Roll-Forming

Two types of parameters have been used in this study. The first type is related to the product's geometry, including FW, ST, and radius of the channel corners. The second type is those related to roll-forming lines, including BAI and I-D. The parameters and their ranges are shown in TABLE I.

The BAI was a categorical parameter, so between 10˚ to 60˚, 5 flower patterns would be defined, including 10˚, 15˚, 20˚, 30˚, and 60˚. Since the strip deformation for the 60˚ BAI was severe and might bring some defects to the product [37], pre-form rolls were designed at the beginning of the roll-forming line to decrease or eliminate any possible edge buckling in the products. A FEM was designed and run based on the time-series NN model results to compare the results with the optimal values extracted from the NN model.

ABAQUS/Explicit 2020 FEM Software was used for all simulations. The rolls were rigid analytical components, while the steel strip was a deformable shell component [38]. The roll geometries were identical to those used in the experiments. The mechanical properties of the steel strips were derived from experimental tensile tests conducted following ASTM E8 Standard [39]. The average mechanical properties of the steel strip are shown in

TABLE **II**.

Since the mechanical properties of the hot-rolled steel strips are the same in all directions, the strip is considered to be isotropic [40]. Fig. 1 shows a FEM of roll-forming a line with a 30˚ BAI that includes 3 forming stands (Pre-form, 30˚, and 60˚ forming rolls).

TABLE I
INPUT PARAMETERS OF COLD ROLL-FORMING PROCEDURE AND THEIR RANGES.

Index	Unit	Bottom range	Top range
I-D	mm	300	500
BAR	degree	10	60
ST	mm	2	3
FW	mm	30	50
BR	mm	1	4

TABLE II
THE STEEL STRIP'S MECHANICAL PROPERTIES.

Yield Strength	Ultimate Tensile strength	Work hardening exponent	Work hardening coefficient	Elongation (%)
202.86	323.59	0.25	581.54	45.53

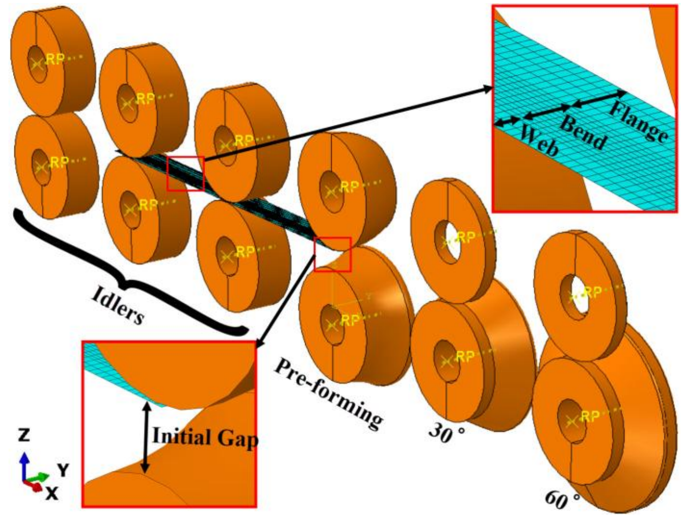

Fig. 1 FEM roll-forming model for 30˚ BAI.

The flat idlers at the first three stands of the simulation are designed to keep the strip at the exact location through-thickness direction, preventing any tail fluctuation when the head is pulled through the forming stands. The tangential contact between the forming rolls and strip was determined based on a modified Columb Friction model with a friction coefficient of 0.1. However, the contact between the idlers and the strip was frictionless[41]. The initial location of the head strip is 1mm farther than the pre-form roll centre in the longitudinal direction to make enough contact between the rolls and strip when the lower roll comes up and squeezes the strip head. The gap between each pair of idlers was equal to ST. In the first phase of the simulation, no contract existed between the strip and the other forming rolls except the upper pre-form rolls that touched the top surface of the strip. The initial gap between the pre-form rolls exceeds the strip's thickness. In the first stage, the lower pre-form roll touches the strip and squeezes about 0.1% of its thickness [42]. It can help the strip to be grabbed fully by the pre-form rollers and then pulled through the forming line with the help of friction, identical to the experimental tests. In the second phase, the rolls rotate and pull the strip through the forming line until the tail of the strip tail comes out of the roll-forming line. Due to the symmetry of the product, only half of the process was simulated. Conforming to the experimental setup, the linear speed of the rolls was 37.85 mm/sec. In addition, the speed was within the range to run the simulations in the quasistatic mode [43]. The mesh was generated by the S4R element with four nodes and five integration points on the strip. The strip contained two sizes of mesh. The first size was used for the element in the web and flange zones, which was a squared element. The second size was used for the element in the bend zone, which had the same length as the one in the web and flange zones but a width three times smaller than the length to accurately simulate the bending deformations [44]. The convergence method was utilised to determine the optimal mesh size with precise results, while the simulation time was optimised [45].

III. Methodology

The proposed methodology of this study is based on the usage of T2FNN and NSGA-II, which are the heart part of this Section. The full factorial investigation of the roll-forming process under a FEM environment is employed in this study to capture the output of the system (required torque and energy consumption) based on the input of the system (bend angle increment at each stand, the internal distance between the stands, strip thickness, channel flange width, and corner radius). Then, two methods (RSM and T2FNN) are used to extract the surrogate model of the system with the same behaviour as the roll-forming process. Then, the optimal process parameters of the roll-forming procedure are extracted using the NSGA-II. At the same time, the extracted surrogate model using T2FNN is employed inside the cost function of NSGA-II. In the final step, the extracted results of NSGA-II (Pareto front distribution of the optimal solutions) are validated via the experiments to prove the efficiency of the proposed model in real-world handling examples.

Fig. 2 represents the schematic representation of the proposed work. It consists of two main steps. The T2FNN is trained and extracted in the first step using the captured datasets in the previous Section. Two T2FNN models are trained and developed in the first step as there are two outputs to be predicted, including maximum required torque and energy usage called T2FNN-Energy and T2FNN-Torque. In the second step, NSGA-II is employed to extract the optimal process parameters, leading to the minimum torque and energy requirement and decreasing the production cost.

It should be noted that the raw datasets cannot be used inside the algorithm unless they sacrifice the model's accuracy. That is why we have discussed data pre-processing as the first subsection in this Section before explaining our proposed T2FNN and NSGA-II. In the following Section, T2FNN and NSGA-II are explained, which are used as the hybrid model to extract the optimal process parameters of the cold roll-forming procedure.

A. *Pre-processing*

The pre-processing of the dataset is used to decrease the system's complexity during the training process of the network to reach higher accuracy. It starts with eliminating the out-of-range data because these data dramatically decrease the accuracy of the network. The main source of these data is the fault in measuring systems. Normalisation is used to allocate the mean and std of the dataset in the rational range and decrease the system's complexity for the network. It has been calculated as follows:

$$n_{x_i} = \frac{x_i - \underline{x}}{\overline{x} - \underline{x}} \tag{2}$$

where $\underline{x}$ and $\overline{x}$ are the minimum and maximum values of the dataset. Also, x_i and n_{x_i} is the i^{th} raw and normalised data. Normalised values are with the interval [0,1]. It should be noted that the normalisation process is implemented for input and output data separately. The final step of the data pre-processing is dividing data into training and testing samples. In this study, 90% and 10% of the dataset are used for the training and testing process of the network. It should be noted that the testing data should not be shown to the system during the training process of the networks.

B. *Type-2 Fuzzy Neural Network*

T2FNN combines a type-2 fuzzy inference system and NN for tuning. The type-2 fuzzy inference system is used in this study to calculate torque and energy consumption in the cold roll-forming procedure called T2FNN-Torque and T2FNN-Energy, respectively. Fig. 3 represents the membership functions of the interval type-2 fuzzy inference system for dealing with the required torque and energy consumption. The captured datasets using the FEM environment shown in [6] are considered for the training purpose of the model. A feedforward NN is also augmented to the type-2 fuzzy inference system model for tuning the model for calculating the required torque and energy consumption. Fig. 4 depicts the schematic of the overall T2FNN structure. In the T2FNN, the considered system

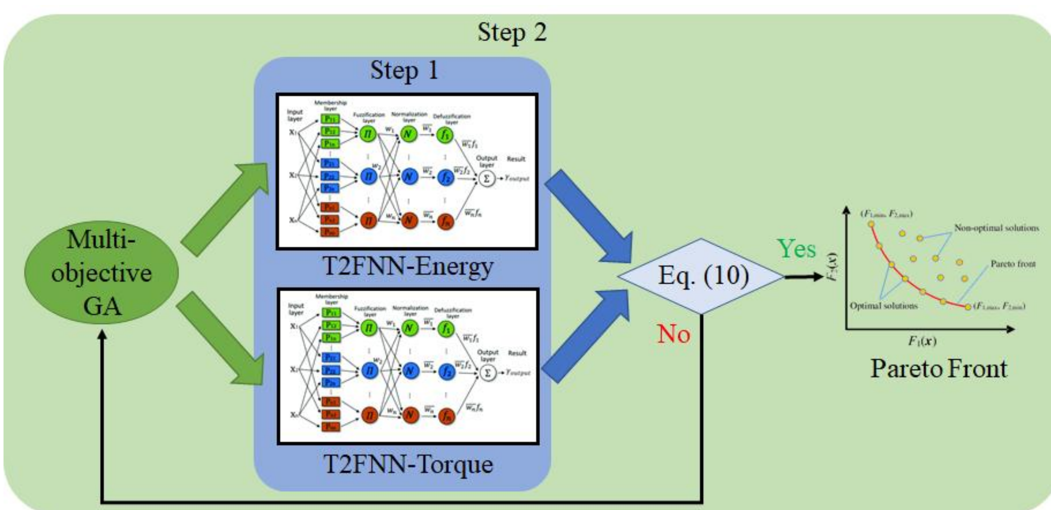

Fig. 2. Schematic representation of the proposed hybrid machine-learning method for calculation of the torque and energy consumption in roll-forming procedure using T2FNN and NSGA-II.

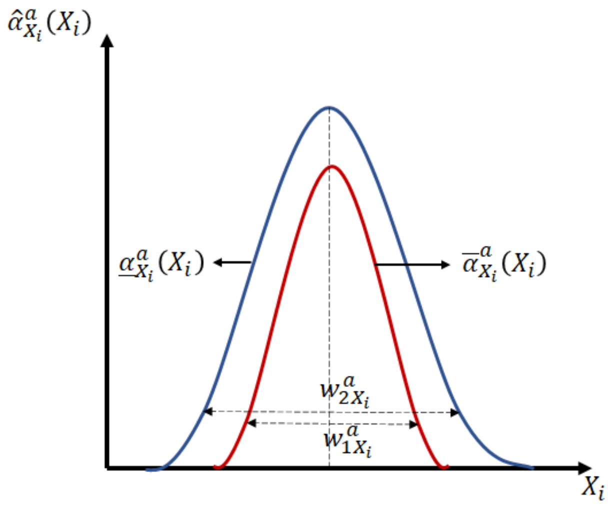

Fig. 3. Type-2 fuzzy inference system membership functions.

will be developed via the several usages of the type-2 fuzzy inference system IF-THEN rules as follows:

Rule a_i: IF $\mathbf{u}_i^* \in Q_u^a$ and $\mathbf{v}_i^* \in Q_v^a$

THEN: $X_i^a = \left[\mathbf{u}_i^{aT}, \mathbf{v}_i^{aT}\right]^T = \hat{r}_{i0}^a + \hat{R}_{u,v}^a\left[\mathbf{u}_i^{*T}, \mathbf{v}_i^{*T}\right]^T = \hat{r}_{i0}^a + \hat{R}_{u,v}^a X_i^*$ (3)

where:

$\hat{R}_{u,v}^a = \left[\hat{r}_{u,v,1}^a, \dots, \hat{r}_{u,v,5}^a\right]^T$ while $\hat{r}_{u,v,n}^a \in \left[\underline{r}_{u,v,n}^a, \overline{r}_{u,v,n}^a\right]$, $n = 1,..,5.$ (4)

Also, $\mathbf{u}_i^*$ and $\mathbf{v}_i^*$ are the reference signals. $a_i = 1, \dots, R_i$ is the number of rules for the systems $i \in \{n, q\}$. Q_u^a and Q_v^a are type-2 fuzzy inference system sets with type-2 fuzzy inference system membership functions.

Therefore:

$$\underline{X}_i^a = \underline{r}_{i0}^a + \underline{R}_{u,v}^a X_i^*$$

$$\overline{X}_i^a = \overline{r}_{i0}^a + \overline{R}_{u,v}^a X_i^* \quad (5)$$

Based on the represented fuzzy sets in Fig. 3, $\hat{\alpha}_u^a(\mathbf{u}_i) = \left[\underline{\alpha}_u^a(\mathbf{u}_i), \overline{\alpha}_u^a(\mathbf{u}_i)\right]$ and $\hat{\alpha}_u^a(\mathbf{v}_i) = \left[\underline{\alpha}_u^a(\mathbf{v}_i), \overline{\alpha}_u^a(\mathbf{v}_i)\right]$ with uncertain mean and standard deviation Gaussian functions, while:

$$0 \le \underline{\alpha}_{X_i}^a(X_i) \le \overline{\alpha}_{X_i}^a(X_i) \le 1 \quad (6)$$

and

$$\underline{\alpha}_{X_i}^a(X_i) = e^{\left(-\frac{1}{2}\left(\frac{X_i - c_{X_i}^a}{w_{1X_i}^a}\right)^2\right)}$$

$$\overline{\alpha}_{X_i}^a(X_i) = e^{\left(-\frac{1}{2}\left(\frac{X_i - c_{X_i}^a}{w_{2X_i}^a}\right)^2\right)} \quad (7)$$

The product of type-2 fuzzy sets leads to the final outputs of the fuzzy rules in each system as follows:

$$\underline{\mu}_{X_i}^a(X_i) = \underline{\alpha}_u^a(\mathbf{u}_i) \times \underline{\alpha}_u^a(\mathbf{v}_i)$$

$$\overline{\mu}_{X_i}^a(X_i) = \overline{\alpha}_u^a(\mathbf{u}_i) \times \overline{\alpha}_u^a(\mathbf{v}_i) \quad (8)$$

So:

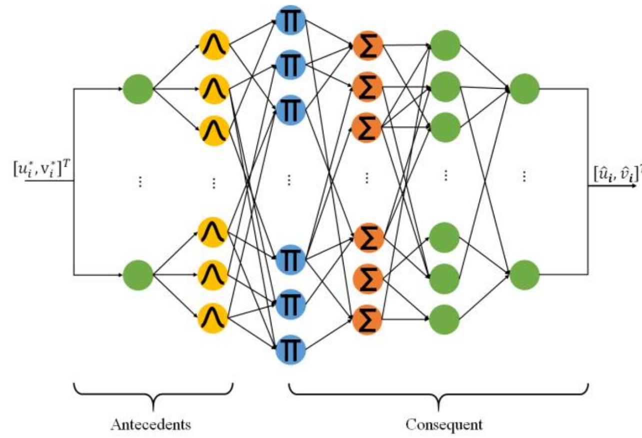

Fig. 4. Schematic representation of the T2FNN.

$$\hat{X}_i = \frac{1}{2}\left(\frac{\sum_{a=1}^{A_i} \underline{\mu}_{X_i}^a(X_i)\underline{X}_i^a}{\sum_{a=1}^{A_i} \underline{\mu}_{X_i}^a(X_i)} + \frac{\sum_{a=1}^{A_i} \overline{\mu}_{X_i}^a(X_i)\overline{X}_i^a}{\sum_{a=1}^{A_i} \overline{\mu}_{X_i}^a(X_i)}\right) \quad (9)$$

The parameters of the type-2 fuzzy inference system are generated by training a NN based on the employed datasets. Takagi–Sugeno fuzzy structure is used in FNN based on the represented rules in Eq. (3). Fig. 4 shows the mechanism of T2FNN using five layers or two main groups, including antecedents and consequent.

C. *Multiobjective Genetic Algorithm: NSGA-II*

In 1995, Deb *et al.* [46] proposed the NSGA algorithm, which combines genetic algorithms with Pareto optimisation to solve Multiobjective optimisation problems. In 2002, the NSGA-II was introduced as an improvement to the NSGA to reduce the system's complexity and increase the calculation pace of the solution via individual stratification. One of the advantages of the NSGA-II is the ability to extract the Pareto front solutions to non-convex problems. Fig. 5 shows the schematic flowchart of the Multiobjective NSGAR-II. The Pareto front distribution of the solution can be extracted by running the NSGA-II once, which is computationally effective. The first step calculates the penalty values using the proposed nonlinear MPC-based AV controller via random weight selections. In the next step, the mutation and crossover of the genetic operator are used to calculate the new population. As the most important part of the NSGA-II, the Elitist strategy extracts the best solution for a newly generated population every cycle. This process is repeated until the number of iterations is satisfied. In the Multiobjective NSGA-II, there is no goal to terminate the optimisation since there is no single objective function. Two functions, crowding distance and non-domain sorting, are used to achieve this task. The non-dominated sorting is used for the cyclic grading purpose of the algorithm. The methodology of the cyclic grading using non-dominated sorting is described as follows:

1. The first non-dominated layer is identified based on the non-dominated set in the group.
2. The non-dominated set is removed from the group.
3. The search is continued in the remaining group.
4. The solutions are sorted based on the dominance relationship.

It should be noted that two objective functions of the current study are calculated based on the mean square error (MSE)

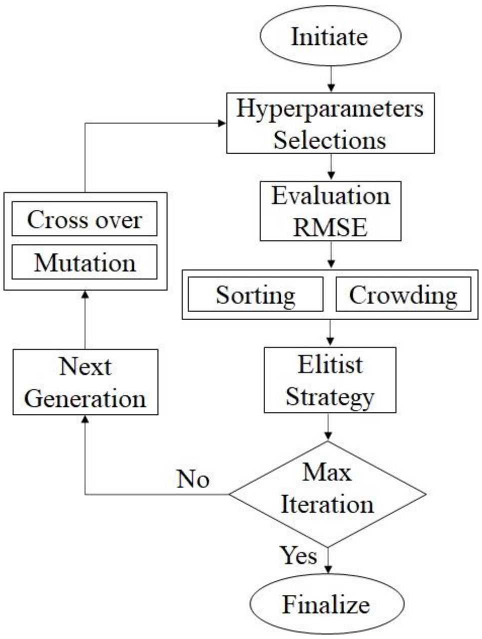

Fig. 5. Flowchart of Multiobjective NSGA-II.

between the actual value (required via experiment FEM) and predicted via proposed T2FNN models as follows:

$$J_{O1}(FW, ST, BAI) = \frac{1}{n}\sum_{i=1}^{n}\left(O1_i - \widehat{O1}_i\right)^2$$
$$J_{O2}(FW, ST, BAI) = \frac{1}{n}\sum_{i=1}^{n}\left(O2_i - \widehat{O2}_i\right)^2 \quad (10)$$

where $O1$ and $O2$ stand for actual torque and energy consumption per length required by FEM. Also, $\widehat{O1}$ and $\widehat{O2}$ are the predicted torque and energy consumption per length required via the proposed T2FNN.

The crowding distance technique extracts the distance between every solution and calculates the surrounding solutions' density. It is calculated by summating the distance between individuals for each objective function. Also, normalisation is employed to prevent the problem that the objectives are on different scales.

IV. Results and Discussions

This Section is composed of two subsections, including verification and validation. In the first subsection, the proposed method is designed and developed under MATLAB software, and the proposed method is in Section III. In the last part of the first subsection, the experiments are verified with the simulation results to reach realistic results as close as possible to the real application. In the second subsection, the results are validated by the previous methods to prove the efficiency of the proposed method.

A. Verification

T2FNN models (including T2FNN-Energy and T2FNN-Torque) have been designed and developed in this study based on the represented model in Section III. The process parameters are BAI (°), I-D (mm), ST (mm), FW (mm) and bending radius (BR mm). As the full factorial study of the process parameters based on the work conducted by Shirani Bidabadi *et al.* [6] has evaluated only two values for I-D and BR, it is impossible to estimate the function's behaviour between these two ranges. Then, we only investigate the optimal solution for I-D = 310 (mm) and BR = 1 (mm). Extraction of the optimal solution for the other arrangement of I-D and BR is possible by using the same proposed methodology in this research. In addition, it should be noted that the BAI (°) parameter should be calculated as a discrete value because it is impossible to manufacture. The rest of the process parameters are controllable. They can be defined based on the extracted optimal solution within the range. The model is trained based on the represented dataset in conducted work by Shirani Bidabadi *et al.* [6]. MATLAB software is used to develop the proposed T2FNN model. The model is compared with the previously developed model by Shirani Bidabadi *et al.* [6] to prove the higher accuracy of the proposed prediction model compared to the previous model (curve fitting models [6]). The networks are trained using 76% of the datasets (82 sets) for the training purpose of the model, and the rest 24% of the dataset (26 sets) is used for testing the model.

An experimental roll-forming setup validated the FEA results extracted from the simulation. One of the U-shaped products, simulated Using Abaqus FEA, was tested experimentally, and the required energy to form the sample was measured. The input parameters in the experimental setup were adjusted the same as those in the FEA simulation. The roll-forming setup is shown in Fig. 6a. As seen in this figure, a dynamic torque meter was used to capture the torque. Then the torque was used to get the forming energy.

The comparison of the graph captured from the torque meter versus the graph extracted from the simulation is shown in Fig. 6b. The torque graph picks a step at the beginning of the forming process when the head of the steel strip goes through each forming stand. It continues until all forming stands are engaged forming process. Then by passing the end of the strip through the forming stand, the torque graph decreases a step until the strip comes out of the roll-forming setup and the torque return to zero.

The difference in torque between the experimental and simulations are less than 7.4%. So, the validation of the simulation is approved since there is a good agreement between the simulated graph and the experimental one. In addition, RSM is a candidate for validating our newly proposed method efficiency as the most recent method by Shirani Bidabadi *et al.* [6].

B. Validation

Fig. 7a-b represents the calculation of the maximum torque and energy consumption per length using the previous curve fitting model and the proposed T2FNN models (including T2FNN-Torque and T2FNN-Energy). Specifically, Fig. 7a shows the calculation of the maximum torque using FEM (reference), T2FNN-Torque (newly proposed method), and RSM (previous method) for 27 datasets with consideration of I-D = 310 (mm) and BR = 1 (mm). Based on the outcomes in Fig. 7a, the correlation coefficient between the FEM and predicted maximum torque using the previous RSM and proposed T2FNN-Torque are 0.9467 and 0.9980, respectively. In the following, Fig. 7b shows the FEM and predicted energy per

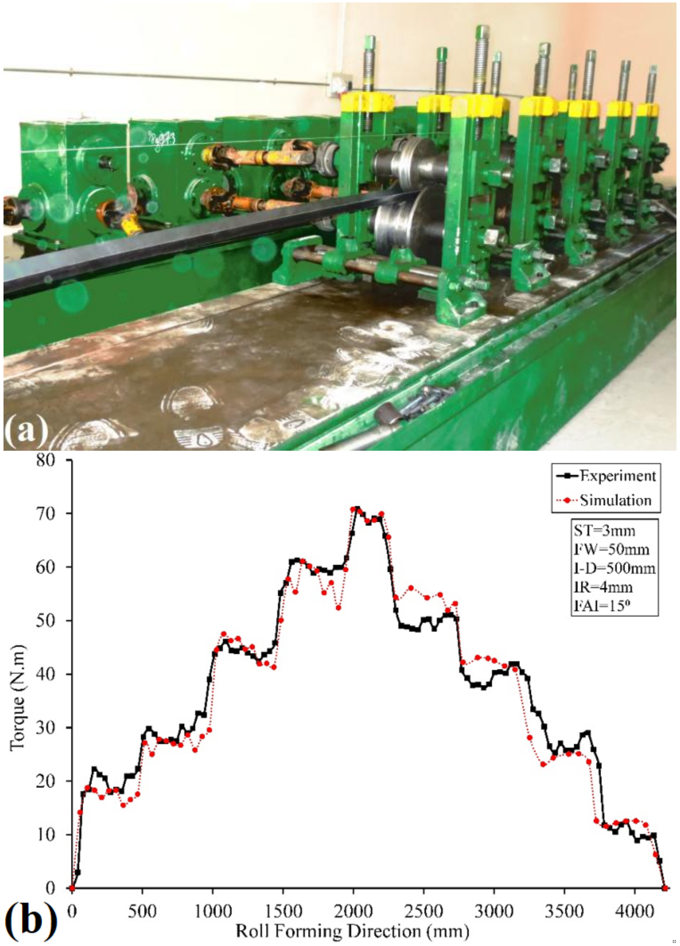

Fig. 6. (a): The experimental roll-forming setup with the torque meter installed; (b): The required torque graph in both simulation and experimental setup for comparison.

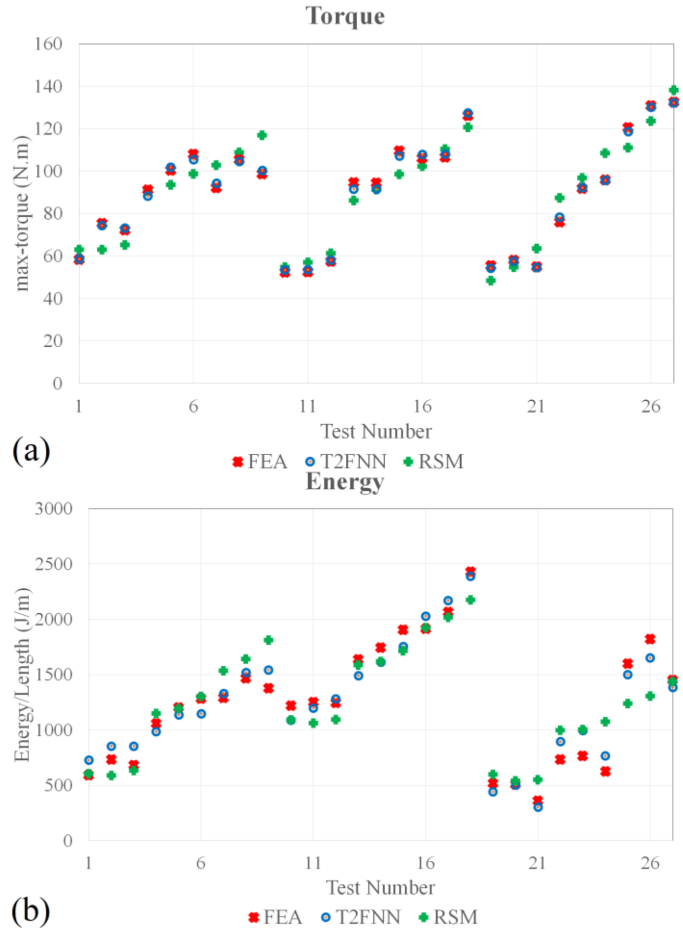

Fig. 7. The FEM and predicted value using previous curve fitting model and the proposed (a): T2FNN-Torque; (b): T2FNN-Energy.

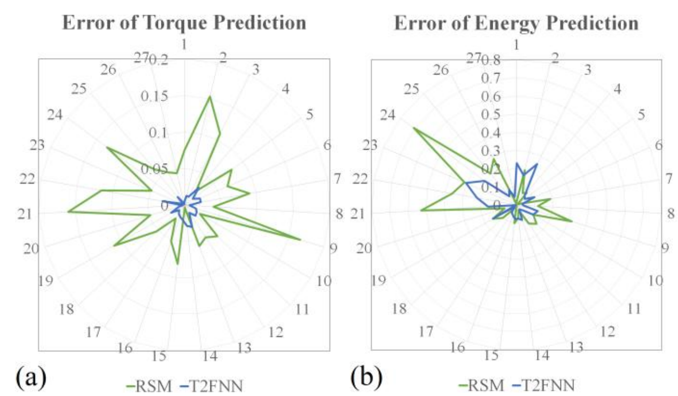

Fig. 8. The error between the FEM and predicted value using previous RSM and the proposed T2FNN models for prediction of (a): maximum required torque; (b): energy consumption per length.

length in the cold roll-forming procedure using previous RSM and proposed T2FNN-Energy methods. The correlation coefficient between the FEM and predicted value using the newly developed (T2FNN-Energy) and previous method (RSM) are 0.9146 and 0.9754 based on the represented outcomes in Fig. 7b, respectively.

Fig. 8a-b shows the error between the reference (FEM) and predicted maximum required torque and energy consumption per length using RSM and T2FNN models, respectively. Based on the represented outcomes in Fig. 8a, the means square error between the FEM and predicted maximum torque using the previous RSM and proposed T2FNN-Torque are 64.3689 (N.m) and 2.5131 (N.m) based on Fig. 8a, respectively. In addition, the root means square error between the FEM and predicted maximum torque using the previous RSM and proposed T2FNN-Torque are 8.0230 (N.m) and 1.5853 (N.m) based on Fig. 8a, respectively. In the following, the mean square error between the FEM and predicted energy per length consumption using previous and newly developed models are 4.7239×10^4 (J/m) and 1.4206×10^4 (J/m) based on the represented outcomes in Fig. 8b, respectively. In addition, the root means square error between the actual and estimated energy per length consumption using previous and new methods are 217.3450 (J/m) and 119.1889 (J/m), respectively.

Fig. 9a-b shows the regression between the FEM and predicted maximum torque of the cold roll-forming procedure for the previous RSM and proposed T2FNN-Torque methods, respectively. The regression between the FEM and predicted torque using the previous and new methods are 0.94667 and 0.99796, respectively. In the following, the regression

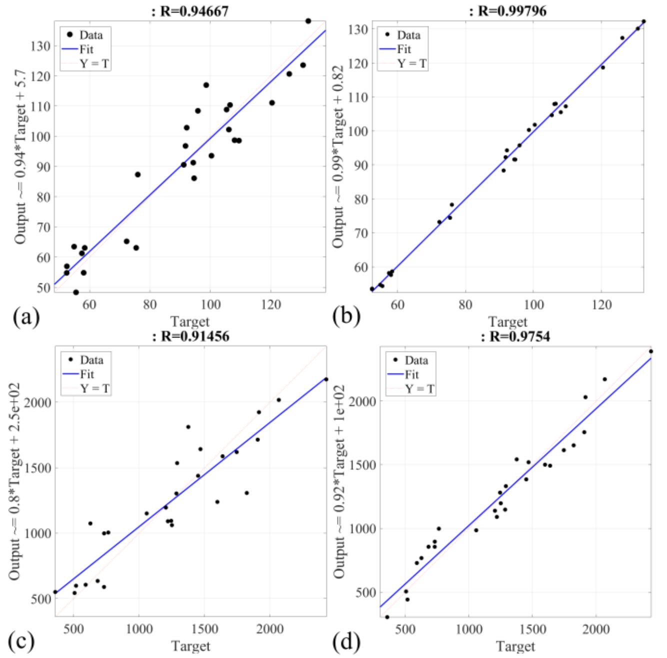

Fig. 9. The regression of the (a): previous algorithm for prediction of the torque; (b): new algorithm for prediction of the torque; (c): previous algorithm for prediction of energy/length consumption; (d): new algorithm for prediction of energy/length consumption

representation of the energy consumption per length using previous and newly proposed methods are shown in Fig. 9c-d, respectively. The regression of the newly proposed T2FNN-Energy is 0.9754, which is higher than the previous method's regression. The training time of the T2FNN-Energy and T2FNN-Torque under usage of a PC with Intel(R) Core(TM) i7-10875H CPU @ 2.30GHz 2.30 GHz are 3.483986 and 1.473459 seconds, respectively.

Figs. 10-11 show the rule surface of the extracted T2FNN-Torque and T2FNN-Energy in calculating the maximum required torque and energy consumption per length, respectively. Based on the represented outcomes in Fig. 10a-c, ST (mm) is the most effective parameter in the calculation of the maximum torque of the process with consideration of I-D =

TABLE III
EXTRACTED RESULTS FOR THE CALCULATION OF TORQUE (N.M) AND ENERGY/LENGTH (J/M) USING THE PROPOSED METHOD AND EXPERIMENTAL STUDY.

No	T2FNN		Experiment		Error	
	Torque	Energy/Length	Torque	Energy/Length	Torque	Energy/Length
1	51.8	467.66	58.0	444.2	12%	5%
2	51.5	473.25	48.9	440.1	5%	7%
3	53.5	460.81	47.0	405.5	12%	12%
4	53.0	462.23	48.2	411.3	9%	11%
5	54.1	458.26	51.9	403.2	4%	12%
6	52.0	466.08	55.1	424.1	6%	9%
7	52.6	463.75	56.8	482.3	8%	4%
8	54.4	457.31	60.9	507.6	12%	11%
9	53.3	461.17	46.9	516.5	12%	12%
10	52.4	464.58	49.7	511.0	5%	10%
11	53.8	459.74	60.2	413.7	12%	10%
12	54.5	456.89	47.9	411.2	12%	10%
13	51.6	470.59	47.4	437.6	8%	7%
14	54.5	314.17	60.4	342.4	11%	9%

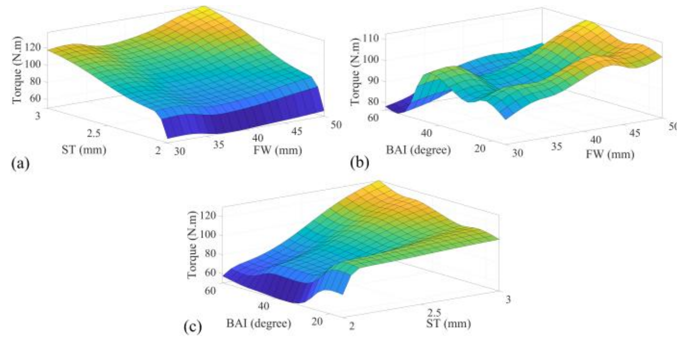

Fig. 10. TFNN rule surface for calculation of torqued based on using the most effective parameter which is ST (mm) and (a): FW (mm); (b): I-D (mm); (c): BAI (°); (d): BR (mm).

310 (mm) and BR = 1 (mm). Based on the represented result in Fig. 10a, the maximum variation of the torque based on the variation of the ST from 2 (mm) to 3 (mm) and fixed FW in 30 (mm) and 50 (mm) are 63.12 (N.m) and 82.45 (N.m), respectively. Based on the represented result in Fig. 10b, the maximum variation of the torque based on the variation of the BAI from 15° to 60° and fixed FW in 30 (mm) and 50 (mm) is 23.56 (N.m) and 18.79 (N.m), respectively. It should be noted that at fixed FW in 30 (mm), the maximum torque is occurred at BAI = 43.42° ≈ 30°. Also, the maximum torque at fixed FW in 50 (mm) occurred at BAI = 41.05° ≈ 30°. The maximum variation of the torque based on the variation of the ST from 2 (mm) to 3 (mm) and fixed BAI in 60° is 72.48 (N.m) based on the shown result in Fig. 10c.

Fig. 11a-c shows the recalculated rule surface of the proposed T2FNN-Energy for calculating the energy consumption per length based on the variation of ST-FW, BAI-FW, and BAI-ST, respectively. Based on the represented result in Fig. 11a, the maximum variation of the energy consumption per length based on the variation of the ST from 2 (mm) to 3 (mm) and fixed FW in 30 (mm) and 50 (mm) is 1105.9 (J/m) and 1316.0 (J/m), respectively. Based on the represented result in Fig. 11b, the maximum variation of the torque based on the variation of the BAI from 15° to 60° and fixed FW in 30 (mm) and 50 (mm) is 957.5 (J/m) and 1376.7 (J/m), respectively. It should be noted that there is an optimum point in the usage of

TABLE IV
EXTRACTED OPTIMAL PROCESS PARAMETERS OF COLD ROLL-FORMING PROCEDURE USING T2FNN AND NSGA-II.

No.	FW (mm)	ST (mm)	BAI (°)
1	31.07634	2.052747	60
2	31.03737	2.067083	60
3	31.10934	2.034493	60
4	31.0801	2.038723	60
5	31.04137	2.028783	60
6	31.0404	2.049341	60
7	31.0744	2.042782	60
8	31.04868	2.026076	60
9	31.07164	2.036086	60
10	31.0681	2.045039	60
11	31.06546	2.032365	60
12	31.03391	2.025205	60
13	31.05239	2.060398	60
14	46.86355	2.001997	60

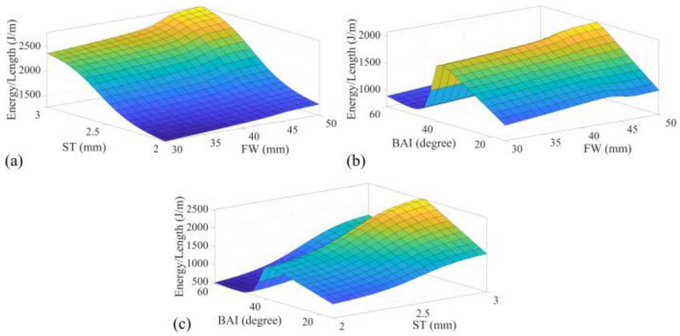

Fig. 11. TFNN rule surface for calculation of torqued based on using the most effective parameter which is ST (mm) and (a): FW (mm); (b): I-D (mm); (c): BAI (°); (d): BR (mm).

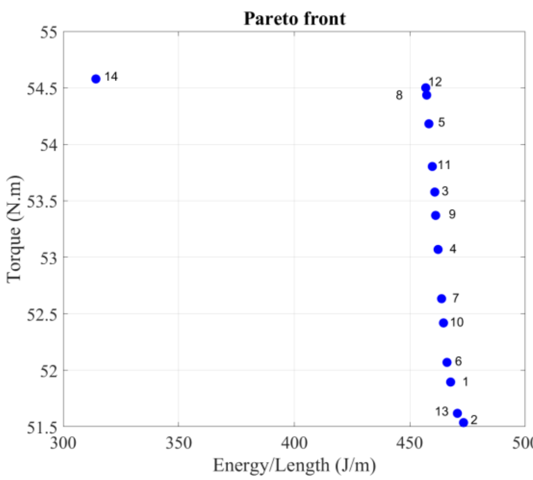

Fig. 12. Pareto front of the extracted optimal solution using NSGA-II in cold roll-forming procedure to extract the optimal maximum torque and energy consumption.

energy per length at fixed FW in 30 (mm) and 50 (mm) and BAI = 41.05° ≈ 30° and BAI = 38.68° ≈ 30°, respectively. Also, the maximum variation of the torque based on the variation of the BAI from 15° to 60° and fixed ST in 2 (mm) and 3 (mm) are 909.4 (J/m) and 1004.1 (J/m) based on the represented result in Fig. 11c, respectively.

In the next step, the proposed T2FNN models for predicting the maximum torque and energy consumption are employed inside the NSGA-II to calculate the optimal solution process parameters of the cold roll-forming procedure. Fig. 12 shows the Pareto front distribution of the optimal solution for the process. In addition, the extracted optimal solutions are mentioned in

TABLE IV.

A series of roll-forming tests were run based on the extracted optimal solution of the proposed T2FNN and NSGA-II to validate the accuracy of the system. The steel strips were cut, and the experimental setup parameters were adjusted using the extracted optimal solutions in Table III. The flange width, strip thickness, and bending radius were used to find the strip width and thickness. Inter-distance between the successive stands, bending angle increment, and bending radius was adjusted on the roll-forming line. Then the roll-forming process was conducted for each sample, and the required torque and energy consumption of the system was captured during the forming process. Finally, the experimental results were compared to the results reported from the proposed T2FNN and NSGA-II. Table IV represents both results extracted from the proposed method and experimental setup. Based on the represented results in Table IV, the proposed method has a very good agreement with the experimental results, and there is less than 9.18% of nonconformance between the data. It proves the precision of the proposed method to predict the energy and torque values in the roll-forming process. It should be noted that the computational time of running the NSGA-II under the previously mentioned PC for the proposed T2FNN models is 125.046223 seconds. It is extracted after 2000 iteration of the proposed T2FNN-Energy and T2FNN-Torque models. However, the computational time of running the NSGA-II without using our proposed surrogate model (FEM) would be huge number of 8000 hours as each experiment under FEM environment takes 4 hours.

A brief description of the results can be represented as follows:

1. The RMSE between the FEM and predicted maximum torque using the newly proposed T2FNN reduced by 80.24% compared to the previously developed RSM.
2. The RMSE between the FEM and predicted energy per length consumption using the newly proposed T2FNN reduced by 45.16% compared to the previously developed RSM.
3. The correlation coefficient between the FEM and predicted maximum torque using the newly proposed T2FNN increased by 5.42% compared to the previously developed RSM.
4. The correlation coefficient between the FEM and predicted energy per length consumption using the newly proposed T2FNN increased by 6.65% compared to the previously developed RSM.

V. Conclusion

In this research, the extracted full factorial results of the previous study in the investigation of the cold roll-forming procedure are used to develop a highly efficient model using T2FNN in calculating the process's maximum torque and energy consumption based on the input production parameters. It should be noted that the input process parameters of the cold roll-forming procedure are BAI at each stand, I-D, ST, and channel FW and corner radius. The proposed model combines type-2 fuzzy sets and a NN. The model is designed and developed under MATLAB software, and the results are compared with the previous model using an RSM. The higher prediction power of the proposed method is proven mathematically in the point of lower mean square error and visually. In the final step, Multiobjective NSGA-II is employed using the extracted T2FNN for extracting the optimal input parameters, which leads to the minimum usage of torque and energy in the production process. As a future study, the idea of transfer learning can be used to implement the deep learning method to extract the most efficient model in modelling the roll-forming process using less amount of dataset [47, 48].

References

1. Shirani Bidabadi, B., et al., *Experimental study of bowing defects in pre-notched channel section products in the cold roll forming process.* The International Journal of Advanced Manufacturing Technology, 2016.
2. Shirani Bidabadi, B., et al., *Experimental investigation of the ovality of holes on pre-notched channel products in the cold roll forming process.* Journal of Materials Processing Technology, 2015. **225**: p. 213-220.
3. Halmos, G., *Roll Forming Handbook*. first ed. 2006, Boca Raton: Taylor & Francis Group.
4. Lindgren, M., *Experimental investigations of the roll load and roll torque when high strength steel is roll formed.* Journal of Materials Processing Technology, 2007. **191**(1-3): p. 44-47.
5. Shirani Bidabadi, B., H. Moslemi Naeini, and R. Azizi Tafti, *Experimental and numerical study of required torque in the cold roll forming of symmetrical channel sections.* Journal of Manufacturing Processes, 2017. **27**: p. 63-75.
6. Shirani Bidabadi, B., et al., *Optimization of required torque and energy consumption in the roll forming process.* International Journal on Interactive Design and Manufacturing (IJIDeM), 2019. **13**(3): p. 1029-1048.
7. Traub, T. and P. Groche, *Energy efficient roll forming processes through numerical simulations.* Journal of Physics: Conference Series, 2018. **1063**: p. 012182.
8. Traub, T., B. Güngör, and P. Groche, *Measures towards roll forming at the physical limit of energy consumption.* The International Journal of Advanced Manufacturing Technology, 2019. **104**(5-8): p. 2233-2245.
9. Davoodi, B., et al. *Numerical and Experimental Investigation of Roll Forces and Torques in Cold Roll Forming of a Channel Section*. in *International conference on advances Materials and processing technologies*. 2010. Paris.
10. Paralikas, J., K. Salonitis, and G. Chryssolouris, *Energy efficiency of cold roll forming process.* The International Journal of Advanced Manufacturing Technology, 2012. **66**(9-12): p. 1271-1284.
11. Paralikas, J., K. Salonitis, and G. Chryssolouris, *Robust optimization of the energy efficiency of the cold roll forming process.* The International Journal of Advanced Manufacturing Technology, 2013. **69**(1-4): p. 461-481.
12. Suvarna, M., et al., *Smart manufacturing for smart cities—overview, insights, and future directions.* Advanced Intelligent Systems, 2020. **2**(10): p. 2000043.
13. Li, J., et al., *Fuel properties of hydrochar and pyrochar: Prediction and exploration with machine learning.* Applied Energy, 2020. **269**: p. 115166.
14. Li, J., et al., *Deep learning accelerated gold nanocluster synthesis.* Advanced Intelligent Systems, 2019. **1**(3): p. 1900029.
15. Durodola, J., *Machine learning for design, phase transformation and mechanical properties of alloys.* Progress in Materials Science, 2022. **123**: p. 100797.
16. Pican, N., F. Alexandre, and P. Bresson, *Artificial neural networks for the presetting of a steel temper mill.* IEEE Expert, 1996. **11**(1): p. 22-27.
17. Cho, S., et al., *A hybrid neural-network/mathematical prediction model for tandem cold mill.* Computers & industrial engineering, 1997. **33**(3-4): p. 453-456.
18. Vannucci, M., V. Colla, and A. Dimatteo, *Improving the estimation of mean flow stress within hot rolling of steel by means of different artificial intelligence techniques.* IFAC Proceedings Volumes, 2013. **46**(9): p. 945-950.
19. Calvo-Rolle, J.L., et al., *A hybrid intelligent system for PID controller using in a steel rolling process.* Expert Systems with Applications, 2013. **40**(13): p. 5188-5196.
20. Dadgar Asl, Y., et al., *Prediction of required torque in cold roll forming process of a channel sections using artificial neural networks.* Modares Mechanical Engineering, 2015. **15**(7): p. 209-214.
21. Lechwar, S., Ł. Rauch, and M. Pietrzyk, *Use of artificial intelligence in classification of mill scale defects.* steel research international, 2015. **86**(3): p. 266-277.
22. Rath, S., P. Talukdar, and A.P. Singh, *Application of artificial neural network for flow stress modelling of steel.* American Journal of Neural Networks and Applications, 2017. **3**(3): p. 36-39.
23. Zhang, C. and P. Jiang, *RFID-driven energy-efficient control approach of CNC machine tools using deep belief networks.* IEEE Transactions on Automation Science and Engineering, 2019. **17**(1): p. 129-141.
24. Xiao, Q., et al., *Meta-reinforcement learning of machining parameters for energy-efficient process control of flexible turning operations.* IEEE Transactions on Automation Science and Engineering, 2019. **18**(1): p. 5-18.
25. Yucel, B., et al., *Mining the correlations between optical micrographs and mechanical properties of cold-rolled HSLA steels using machine learning approaches.* Integrating Materials and Manufacturing Innovation, 2020. **9**(3): p. 240-256.
26. Woo, Y.Y., et al., *Application of support vector regression and genetic algorithm to reduce web warping in flexible roll-forming process.* Journal of Manufacturing Science and Engineering, 2021. **143**(3).
27. Xiao, Q., et al., *Energy efficiency modeling for configuration-dependent machining via machine learning: A comparative study.* IEEE Transactions on Automation Science and Engineering, 2020. **18**(2): p. 717-730.
28. Soleymani, M., M. Khoshnevisan, and B. Davoodi, *Prediction of micro-hardness in thread rolling of St37 by convolutional neural networks and transfer learning.* The International Journal of Advanced Manufacturing Technology, 2022: p. 1-14.
29. Xia, J., et al., *Using feed-forward perceptron Artificial Neural Network (ANN) model to determine the rolling force, power and slip of the tandem cold rolling.* ISA transactions, 2022.
30. Zhu, M., et al., *Three Dimensional Metal-Surface Processing Parameter Generation Through Machine Learning-Based Nonlinear Mapping.* Tsinghua Science and Technology, 2023. **28**(4): p. 754-768.
31. Cao, H., et al., *Research on the Curvature Prediction Method of Profile Roll Bending Based on Machine Learning.* Metals, 2023. **13**(1): p. 143.
32. Chen, Z., et al., *Multi-faceted modelling for strip breakage in cold rolling using machine learning.* International Journal of Production Research, 2021. **59**(21): p. 6347-6360.
33. Hou, Y., Y. Wu, and H. Han, *Multi-Objective Differential Evolution Algorithm Balancing Multiple Stakeholders for Low-Carbon Order Scheduling in E-Waste Recycling.* IEEE Transactions on Evolutionary Computation, 2023.
34. Ding, Z., et al., *NSGA-II Model-Based Dielectric Frequency Response Parameters for Aging and Moisture Analysis of Transformer Insulation.* IEEE Transactions on Instrumentation and Measurement, 2022. **71**: p. 1-10.
35. Mousavi, S., et al., *Directed Search: A New Operator in NSGA-II for Task Scheduling in IoT Based on Cloud-Fog Computing.* IEEE Transactions on Cloud Computing, 2022.
36. Xing, C., et al., *Robust Optimization of Energy-Saving Train Trajectories under Passenger Load Uncertainty Based on p-NSGA-II.* IEEE Transactions on Transportation Electrification, 2022.
37. Kasaei, M.M., et al., *Flange Wrinkling in Flexible Roll Forming Process.* Procedia Engineering, 2014. **81**: p. 245-250.
38. Shirani Bidabadi, B., et al., *Experimental and numerical study of bowing defects in cold roll-formed, U-channel sections.* Journal of Constructional Steel Research, 2016. **118**: p. 243-253.
39. ASTM, *Standard Test Methods for Tension Testing of Metallic Materials [Metric]*, in *E0008_E0008-21*. 2022, ASTM. p. 30.
40. Tajik, Y., et al., *A strategy to reduce the twist defect in roll-formed asymmetrical-channel sections.* Thin-Walled Structures, 2018. **130**: p. 395-404.
41. Shirani Bidabadi, B., *Numerical and experimental study of transforming the hole in cold roll forming process of pre-notch section*. 2013, MS Thesis, Department of Mechanical Engineering, Tarbiat Modares University ….
42. Safdarian, R. and H. Moslemi Naeini, *The effects of forming parameters on the cold roll forming of channel section*, in *Thin-Walled Structures*. 2015. p. 130-136.
43. Tehrani, M.S., et al., *Localised edge buckling in cold roll-forming of symmetric channel section.* Thin-Walled Structures, 2006. **44**(2): p. 184-196.

44. Shirani Bidabadi, B., et al., *Investigation of over-bending defect in the cold roll forming of U-channel section using experimental and numerical methods.* Proc IMechE Part B: J Engineering Manufacture, 2022. **236**(10): p. 1380–1392.
45. Abedian, A., B. Shirani Bidabadi, and R. Shateri, *Numerical and experimental study of open die forging process design for producing heavy valves.* International Journal on Interactive Design and Manufacturing (IJIDeM), 2017.
46. Deb, K., et al., *A fast and elitist multiobjective genetic algorithm: NSGA-II.* IEEE transactions on evolutionary computation, 2002. **6**(2): p. 182-197.
47. Kabir, H.D., et al., *Spinalnet: Deep neural network with gradual input.* IEEE Transactions on Artificial Intelligence, 2022.
48. Kumar, K., et al. *SpinalXNet: Transfer Learning with Modified Fully Connected Layer for X-Ray Image Classification*. in *2021 IEEE International Conference on Recent Advances in Systems Science and Engineering (RASSE)*. 2021. IEEE.